

Parametric Study of Stationary Body Facing its Own Wake in a High Speed Compressible Rotating Flow

T.K. Bera

Chemical Technology Group, Bhabha Atomic Research Centre, Mumbai - 400085, INDIA.
E-mail: tkbera@barc.gov.in

ABSTRACT

Strongly rotating flow which is characterized by steep exponential density rise in the radial direction provides unique opportunity to analyze high speed flow for longer durations as compared to conventional shock tunnels, free-piston shock tunnels and expansion tubes. Cylinder wall speed and the position of the test specimen decide the value of upstream Mach number for such studies. Experimental investigations were performed to understand the effect of these two parameters on the stagnation pressure and temperatures of a stationary body placed in high speed rotating flow. A stationary body when placed in a rotating flow field faces its own wake and as a result produces slowdown. In this paper a radial entropy factor, R_{ef} has been introduced to account for the entropy generation which not only depends on Mach number but also on the density of the flow which varies exponentially with respect to radial position. A simple mathematical model has also been developed to understand the complex effects of wall speed and stationary body's radial position on this slowdown. The model has been validated with the experimental data and extended so that stagnation pressure and temperature are predicted with good accuracy.

Key words: Entropy, High speed flow, Radial entropy factor, Rotating flow, Slowdown, Stagnation pressure, Stagnation temperature, Wake

Nomenclature

A_{sq}	= square of ratio of rotational speed to thermal speed
M	= Mach number
p	= absolute pressure (Pa)
R	= ratio of universal gas constant to molecular weight
R_{ef}	= radial entropy factor
ΔS	= entropy generation
T	= temperature (K)

Subscripts

<i>amb</i>	= ambient
<i>avg</i>	= average
<i>axis</i>	= at the axis of cylinder
<i>fs</i>	= free stream condition
<i>H</i>	= header
<i>max</i>	= maximum
<i>o</i>	= stagnation condition
<i>r</i>	= at radius r
<i>ref</i>	= reference value
<i>SB</i>	= solid body
<i>stag</i>	= condition of stagnation
<i>wall</i>	= at the cylinder wall

Greek symbols

γ	= ratio of specific heats
δ	= parameter determined numerically
Ω	= angular velocity ($=2\pi \times \text{frequency of rotation}$)

1. INTRODUCTION

Rotating flows are of vital importance for a number of engineering design applications where fluid flow happens inside rotating machines. These flows are of considerable interest in applications such as centrifugal separators, hydrodynamic bearings, rotating machinery, rotary heat exchangers, etc. High speed flow is characterized by i) thin shock layer with shock very close to the body, ii) entropy layer resulting in vortical flow, iii) thick viscous layer resulting in merged shock-viscous layer, iv) high temperature and real gas effects. In rotating flows the inward pressure gradient is balanced by the centrifugal force. Development of re-entry vehicles, aero-assisted orbital transfer vehicle (AOTV), single stage to orbit (SSTO), scramjet technologies, etc. requires experimental research in ground based test facilities to understand high speed flow, predict aerodynamic properties and validate theoretical research and simulation codes.

In most of the ground based test facilities the high speed flows are produced for short duration using impulse facilities with test duration ranging about 0.05–10 ms. These impulse test facilities include free-piston shock tunnel and expansion tubes where test is carried out for short duration using high enthalpy slug of test gas. Because of short test duration there are difficulties associated with process of data acquisition. Compared to this strongly rotating flow in high speed cylinder provides unique opportunity to analyze high speed flow for a longer duration. For rapidly rotating viscous compressible flows the gas is held under rigid-body rotation. The effective acceleration in the radial direction may be of the order of 1 million g (Earth's gravitational acceleration). Such a flow is characterized by an exponential density and pressure rise in the radial direction towards the periphery with extremely thin thermal, viscous boundary layers and a rarefied inner core [1, 2].

In a rotating vessel same Mach number can be obtained either i) when Pitot test specimen is placed at lower radial position with vessel operating at higher speed, or ii) when Pitot test specimen is placed at higher radial position but vessel operates at lower speed. So, radial location of test specimen and the cylinder wall speed form two important parameters on which the study has been performed. The prediction of stagnation pressure and temperature is quite complicated in a high speed rotating flow due to i) exponential rise in density with respect to radius, ii) the test specimen facing its own wake. In this paper experimental studies were conducted to observe the variation in temperature and pressure at the test specimen for different radial locations and cylinder wall speeds.

Section 2 describes the experimental setup and its methodology. Section 3 describes the study using computational fluid dynamics solver. Section 4 gives the details of development of a mathematical model which can predict various features of the flow. Section 5 gives the conclusion.

2. EXPERIMENTAL METHODOLOGY

2.1. Test facility

The rotating high speed test facility as shown in Fig. 1, comprises of a high speed rotating vessel in a stationary outer vessel. In order to reduce the drag the gap between the inner rotating vessel and outer stationary vessel is kept under evacuated condition using vacuum pump. For this purpose diffusion pump and rotary pump are provided in the outlet side in order to operate the vessel under sub-atmospheric condition and keeping the fluid in vapor condition. Motive gas with lower speed of sound is the preferred choice so as to operate the test setup at supersonic speed. The vessel is also provided with inlet and outlet pipes for fluid intake and exit.

The experimental procedure consists of evacuating the test facility containing the test specimen inside a rotating high speed cylinder. The motive gas is fed through control valve. The holdup of gas in the vessel can be controlled by changing the inlet and exit flow condition. The flow of motive gas is measured using accurate thermal mass flow meter and pressure measurement is carried out using capacitance based pressure gauge. Temperature measurements were done using resistance temperature detectors as shown in Fig. 2. All the temperatures are reported in Kelvin, fr e.g. T_{amb} represents the ambient temperature in Kelvin. Header pressure, P_H is measured before the motive gas is fed into the system. The test facility is provided with pre-calibrated specimen movement assembly to aid the placement of the specimen at the

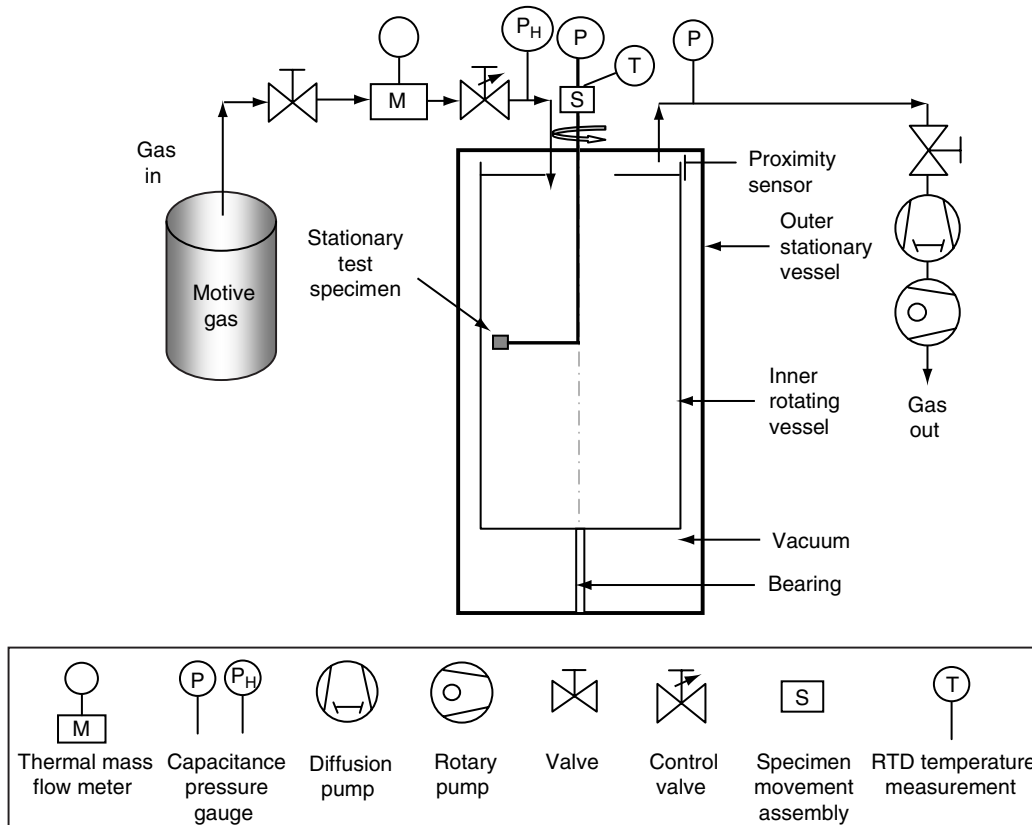


Figure 1. Rotating high speed test facility.

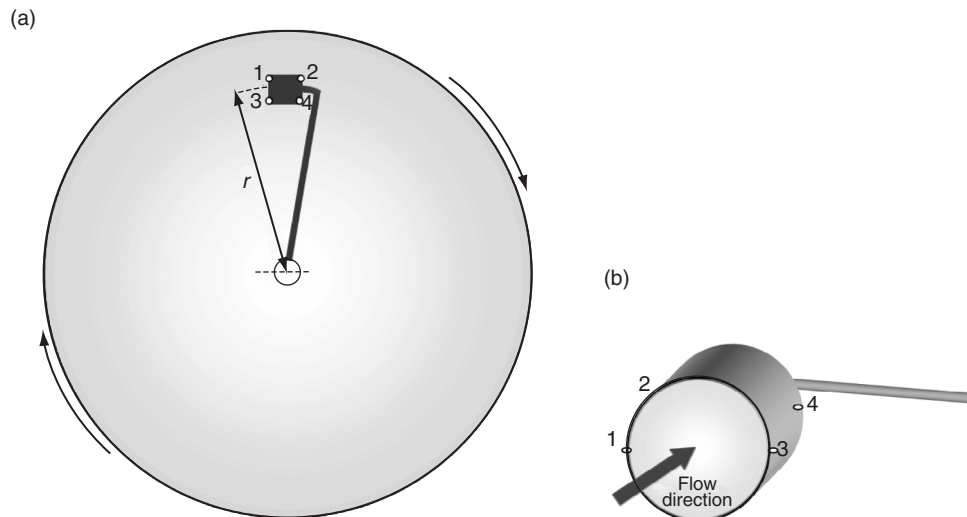


Figure 2(a). Cylindrical Pitot tube placed at radial position r_s ; 2(b) Cylindrical Pitot tube with four embedded temperature sensors.

desired radial position in a running test facility. Data acquisition system collects the temperature, pressure and other relevant data under steady state condition. The data acquisition rate is ~ 20 events /second. The experiments were repeated for different test specimen dimensionless radial positions (varying from 0.91 to 0.951) and with various speeds of rotation of the cylinder (corresponding to wall Mach numbers varying from 4.9 to 6.6).

2.2. Experimental measurement

Test specimen comprises of a cylindrical Pitot tube with embedded temperature sensors as shown in Figure 2a. The Pitot tube is placed at a radial distance of r_s measured from the centre of the tube to the axis of the rotating vessel. The cylindrical Pitot tube is embedded with four temperature sensors as shown in Figure 2b. Sensors 1, 3 are positioned diametrically opposite near the mouth of the Pitot tube. Sensors 2, 4 are placed behind sensors 1 and 3 respectively. The data from the front two sensors have been used in this study. Other two sensors provide data which is useful in calculation of heat transfer through the test specimen. Heat transfer analysis is not in the scope of this paper. The Pitot tube measures the temperature as well as stagnation pressures for different dimensionless radial position given by the ratio of the test specimen tip radius to the radius of the rotating vessel. Proximity sensor was used for frequency measurement of the cylinder wall. The zone in which Pitot tube is inserted in a cylinder rotating at high speed falls in supersonic/hypersonic regime. The mere insertion of a Pitot tube creates a shock and slows down the flow. In this rotating cylinder, such a wake stream rotates back in the cylinder and becomes the upstream for the Pitot tube. After the signal travels a few cycles about the cylinder, a steady is reached with a slowdown in upstream velocity. Fig. 3 shows the temperature on test specimen tip with respect to radial position for different Mach numbers. Sonic speed at T_{amb} is known for the motive gas. So, the Mach number for the wall can be calculated. Figure 4 gives the stagnation pressure and radial position at three different Mach numbers.

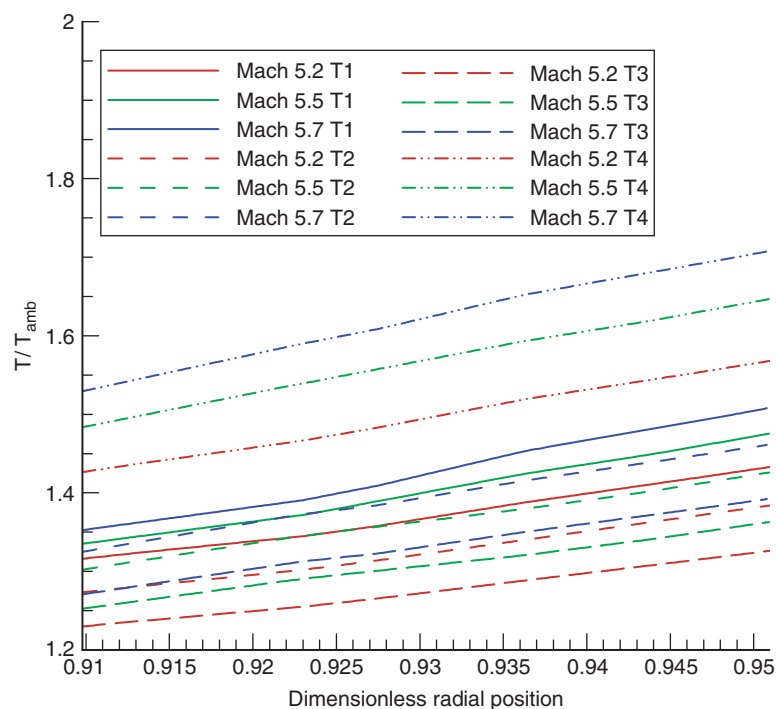


Figure 3. Dimensionless temperature plotted against dimensionless radial position for different Mach numbers.

2.3. Error estimation

Error accumulated in different measuring instruments leads to erroneous output value from the experimental setup. The process data measurement instruments used are absolute pressure transducer, temperature sensors, proximity sensor for frequency measurement, thermal mass flow meter for flow rate measurement.

The capacitance absolute pressure transducer is designed specifically to meet the needs of vacuum process systems where environmental and process conditions are particularly demanding. The unit is

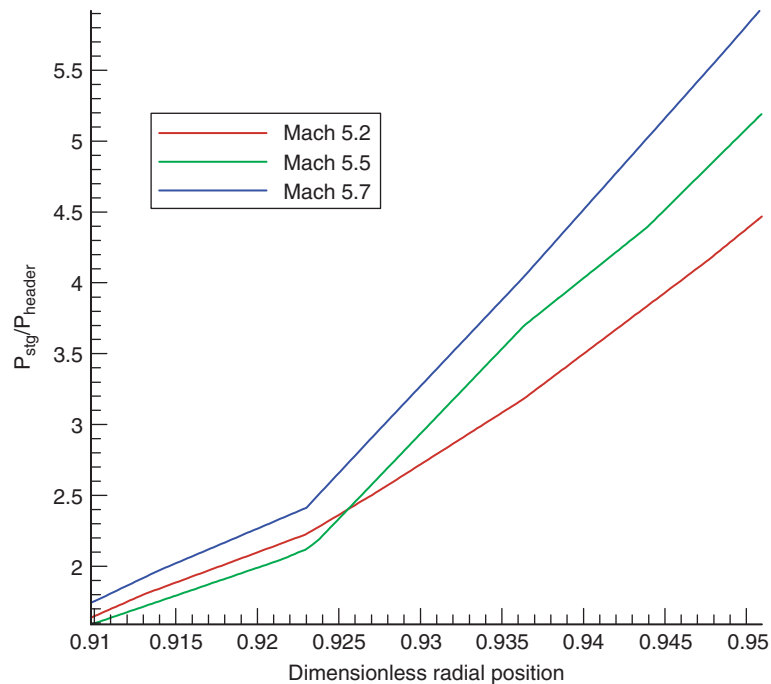


Figure 4. Dimensionless stagnation pressure variation with radial position at different Mach numbers.

capable of measuring pressure at ambient temperatures of 15°C to 40°C. All pressure transducers require initial and periodic zero adjustments. To achieve the full dynamic range specified for the transducer, the zero adjustment must be made at a pressure less than the transducer's resolution (0.001% of full scale). The accuracy of the measurement is $\pm 0.12\%$ of full scale reading.

The device used for temperature measurement is PT100, the platinum resistance temperature detector. The principle of operation is to measure the resistance of a platinum element. The most common type (PT100) has a resistance of 100 ohms at 0°C and 138.4 ohms at 100°C. The relationship between temperature and resistance is approximately linear over a small temperature range and its measurement accuracy is limited within $\pm 1.0\%$. For precision measurement, it is necessary to linearize the resistance to give an accurate temperature. The most recent definition of the relationship between resistance and temperature is International Temperature Standard 90 (ITS-90).

The frequency of rotation is measured using eddy current proximity sensor. Voltage pulse train corresponds to rotation speed. The period of this voltage pulse train is measured using counters. To ascertain the accuracy and resolution over whole measurement range dynamic sub ranging is used. The resolution of frequency measurement is 0.1 Hz. The range of present proximity sensor 5–1000 Hz and accuracy of measurement is 0.1 Hz.

Thermal mass flow meter works on the principle of thermal conductivity of the gases. It can function at ultra low vacuum as its functioning is independent of pressure. However the accuracy is limited to 1% of the full scale reading which is free from thermal drift. Mass flow meter is one of the major sources of error and therefore requires calibration in regular intervals.

3. COMPUTATIONAL FLUID DYNAMICS OF STATIONARY BODY IN HIGH SPEED ROTATING FLOW

Flow past a rigid circular cylinder has been one of the classical problems of fluid dynamics. Extensive studies are reported in literature on linear flows past such blunt bodies [3, 4]. However, only a few studies have been reported of rotating flows past blunt bodies. In case of rotating flows, a flow slowdown is caused by the presence of the stationary body (or the test specimen). The body faces its own wake which strongly affects the flow inside the domain. At high speeds of rotation the average temperature of the gas rises due to the heated wake. Thus, linear flows past stationary blunt bodies are quite different from rotating flows.

Aoki [5, 6] carried out 3-D numerical simulations of the Navier-Stokes equations using a grid of $51 \times 31 \times 21$. Aoki observed that shock pattern greatly depends on the centrifugal force. Matsuda and Tamura [7], Matsuda *et al.* [8] carried out 3-D Euler calculation using Roe scheme for a cylindrical stationary body under strong rotation using H-H-H grid of $90 \times 30 \times 46$. Matsuda *et al.* [8] observed a large size local subsonic pocket near the stationary body. Roberts [9] also found a large density perturbation with strong radially inward flow. Mahendra *et al.* [10] carried out study of rarefied rotating flow past stationary body and observed vortex ahead due to baroclinic effect because of entropy gain as pressure and density are no longer isentropically related.

In this paper computational fluid dynamics (CFD) studies were carried out for high speed flow past a stationary circular cylinder placed in a rotating annulus. In order to simulate test specimen a detailed CFD study was carried out with inner and outer cylinders rotating at constant angular velocity, while the test specimen (body) is stationary. In a high speed rotating flow a steep exponential density rise in the radial direction towards the periphery is present which leaves a thin boundary layers and a rarefied inner core. Navier Stokes equation does not hold in the rarefied inner core, so CFD computations are avoided in this region by taking an inner rotating cylinder. The test specimen is assumed to be a circular cylinder for computational ease. Fig. 5 shows the geometry of the flow domain and mesh, Fig. 6 shows the enlarged view of mesh near stationary cylinder. Mesh size was chosen so that thin boundary layers get properly resolved. In the present simulations a FVM solver was used which uses KFVS for inviscid split flux evaluations [11, 12]. Solution is updated in time using a two step operator splitting procedure. In the first step, explicit time update is performed for the conserved variables using the inviscid KFVS split fluxes. Second step then solves an implicit time correction for the primitive variables using the viscous terms.

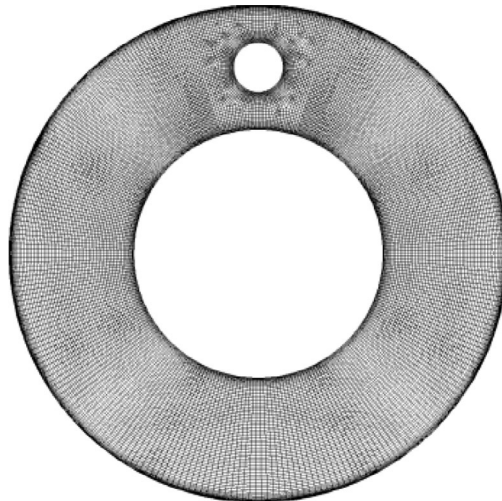


Figure 5. Flow domain geometry and mesh.

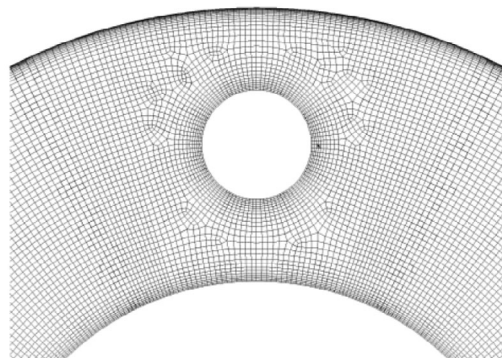


Figure 6. Enlarged view of mesh near stationary cylinder.

The solver was validated earlier for rotating flows problems [13]. Initially, the motive fluid is at rest, while the density and temperature were constant values. The boundary conditions on the stationary body was adiabatic no slip wall, whereas for the rotating cylinder the boundary conditions were isothermal no slip rotating wall. The high centripetal force in the radial direction inside the rotating cylinder helps in maintaining the flow as laminar, with exceptions to zones near stationary body where local turbulence may arise for which Reynolds stress model is the approach.

CFD studies revealed that there are three steady vortices near to the body. One of these three vortices is in front of the body while the other two asymmetric vortices are observed behind the body [13]. Since the stationary body faces its own wake there is a flow slowdown caused by the body. This slowdown increases with the speed and the body wake is observed to have higher temperatures with increasing speed. As seen in Fig. 7 a large subsonic pocket with a vortex ahead of the stationary body was observed. At lower speed the subsonic region becomes large sized by spreading against the direction of

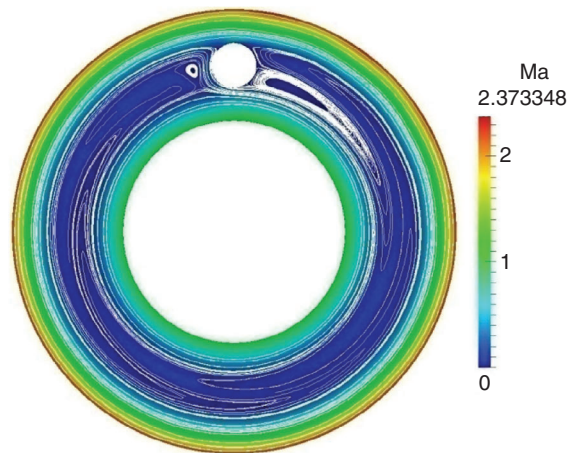


Figure 7. Mach contour showing slowdown with vortex structure.

the oncoming flow as well as towards the radial direction. The vortex in front at higher speed occurs because of baroclinic term. If $\nabla\rho \propto \nabla p \neq 0$ then, this baroclinic effect creates the vorticity because of entropy gain as pressure and density are no longer isentropically related [10].

The results from a large number of CFD simulations performed, reveals that the slowdown due to body wake follows a simple relationship $\Omega_r = \Omega_{ref} \times \left(\frac{r}{r_{max}}\right)^\delta$ where Ω_r is the angular velocity of local rotation at the radial location r of the body and Ω_{ref} is a reference angular velocity near to wall of the cylinder. r_{max} is radius of the cylindrical vessel and δ is a constant which depends on the shape and geometry of the body which is to be determined experimentally. This relationship is the result of slowdown and due to body facing its own wake inside a high speed rotating flow.

4. DEVELOPMENT OF A MATHEMATICAL MODEL

When the vessel is rotated at a very strong speed the gas is under rigid body rotation and the pressure at any radial position r can be given [1, 2] as

$$\frac{p_r}{p_{axis}} = \exp\left(\frac{(\Omega r)^2}{2RT}\right) = \exp(A_{sq}). \quad (1)$$

Where Ω is the angular velocity in radians per second, R is the specific gas constant, and T is the gas temperature. The factor A_{sq} is the ratio of the square of the rotational speed with the thermal speed of the molecules. The Rayleigh Pitot formula for normal shock [14] can be written as

$$\frac{P_{stag}}{p(r)} = \left(\frac{\gamma + 1}{2} M^2 \right)^{\frac{\gamma}{\gamma - 1}} \left(\frac{\gamma + 1}{2\gamma M^2 - (\gamma - 1)} \right)^{\frac{1}{\gamma - 1}} \quad (2)$$

Where M is the upstream Mach number, γ is ratio of specific heats, $p(r)$ is the pressure at radial position r before the shock. The entropy generation, ΔS due to shock can be written [14] as

$$\exp\left(\frac{-\Delta S}{R}\right) = \left[\frac{(\gamma + 1)M^2}{(\gamma - 1)M^2 + 2} \right]^{\frac{\gamma}{\gamma - 1}} \left[\frac{(\gamma + 1)}{2\gamma M^2 - (\gamma - 1)} \right]^{\frac{1}{\gamma - 1}} \quad (4)$$

Equation 4 can be written in form of stagnation quantities as follows

$$\exp\left(\frac{-\Delta S}{R}\right) = \left[\frac{T_r}{T_{stag}} \right]^{\frac{\gamma}{\gamma - 1}} \left[\frac{P_{stag}}{P_r} \right] \quad (5)$$

In the rotating vessel same stagnation pressure can be observed either i) when Pitot test specimen is placed at lower radial position with vessel operating at higher speed, or ii) when Pitot test specimen is placed at higher radial position but vessel operates at lower speed. Since the gas density varies exponentially towards the peripheral wall hence the Pitot tube may face the gas of different density even at same Mach number at two different radial positions. Hence there is a need for a measure of entropy generation when the Pitot tube is placed in a rotating flow. Equation 6 shows the radial entropy factor which is a measure of entropy generation at a particular pressure of inlet stream at Pitot tube's radial location r .

$$R_{ef} = \ln \left[\exp\left(\frac{-\Delta S}{R}\right) P_r \right] = \ln \left[\left[\frac{T_r}{T_{stag}} \right]^{\frac{\gamma}{\gamma - 1}} P_{stag} \right] \quad (6)$$

This p_r can be derived from two approaches : i) first being the case where the mass of gas in the cylinder is assumed constant, ii) second being the case where the axis pressure of the cylinder remains constant. The average pressure p_{avg} (a measure of mass inside the cylinder) can be simplified for low axis pressure as

$$p_{avg} = p_{axis} \left[\frac{\exp(A_{sq,wall}) - 1}{A_{sq,wall}} \right] \approx \frac{p_{wall}}{A_{sq,wall}} \quad (7)$$

For the situation where mass is held constant ($p_{avg} = \text{constant}$), p_r in equation 6 can be written as

$$p_r = \frac{p_{avg} A_{sq,wall}}{\exp(A_{sq,wall} - A_{sq,r})} \propto \frac{A_{sq,wall}}{\exp(A_{sq,wall} - A_{sq,r})} \quad (8)$$

Radial entropy factor $R_{ef,1}$ for this case can be written as follows

$$R_{ef,1} = \ln \left(\exp\left(\frac{-\Delta S}{R}\right) P_r \right) = \ln \left\{ \left[\frac{(\gamma + 1)M^2}{(\gamma - 1)M^2 + 2} \right]^{\frac{\gamma}{\gamma - 1}} \left[\frac{(\gamma + 1)}{2\gamma M^2 - (\gamma - 1)} \right]^{\frac{1}{\gamma - 1}} \frac{A_{sq,wall}}{\exp(A_{sq,wall} - A_{sq,r})} \right\} \quad (9)$$

Similarly for the second case where axis pressure is assumed constant, p_r can be cast into the form as below.

$$p_r = p_{axis} \exp(A_{sq,r}) \propto \exp(A_{sq,r}). \tag{10}$$

Hence a second form of radial entropy factor $R_{ef,2}$ can be written as follows

$$R_{ef,2} = \ln \left(\exp \left(\frac{-\Delta S}{R} \right) p_r \right) = \ln \left\{ \left[\frac{(\gamma + 1)M^2}{(\gamma - 1)M^2 + 2} \right]^{\frac{\gamma}{\gamma - 1}} \left[\frac{(\gamma + 1)}{2\gamma M^2 - (\gamma - 1)} \right]^{\frac{1}{\gamma - 1}} \right\} + A_{sq,r}. \tag{11}$$

The factors $R_{ef,1}$ and $R_{ef,2}$ indicate the entropy generation due to shock in rotating flow field which not only depends on the Mach number of the shock but also on the pressure of the flow which varies exponentially with respect to its radial placement. The variation of factors $R_{ef,1}$ and $R_{ef,2}$ with respect to Mach number tells about the holdup change in the vessel with respect to change in vessel rotating speed is shown in Fig. 8. In Fig. 9 the contour of this factor is plotted with respect to Mach number and dimensionless radial position.

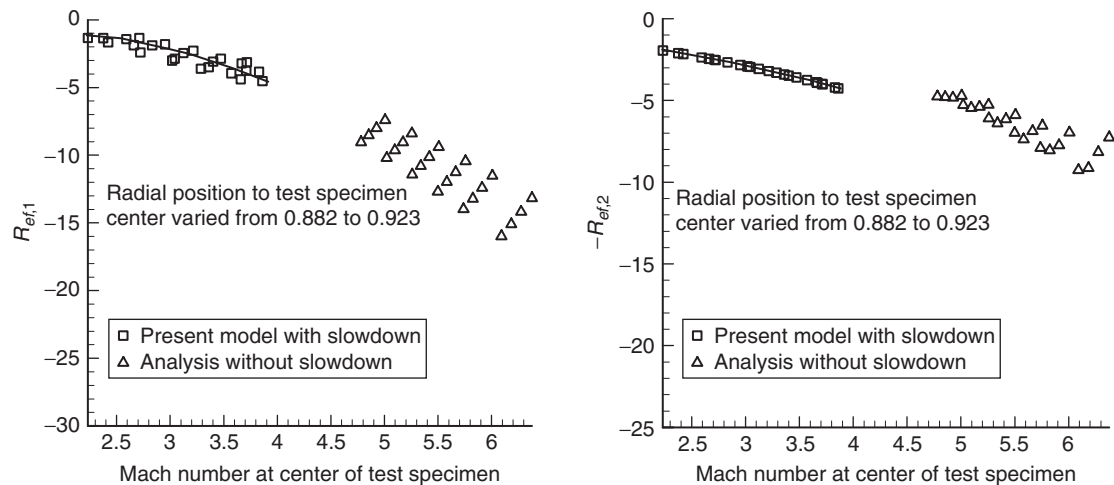


Figure 8. Radial entropy factors with respect to Mach number at the radial position of the test specimen, with and without slowdown.

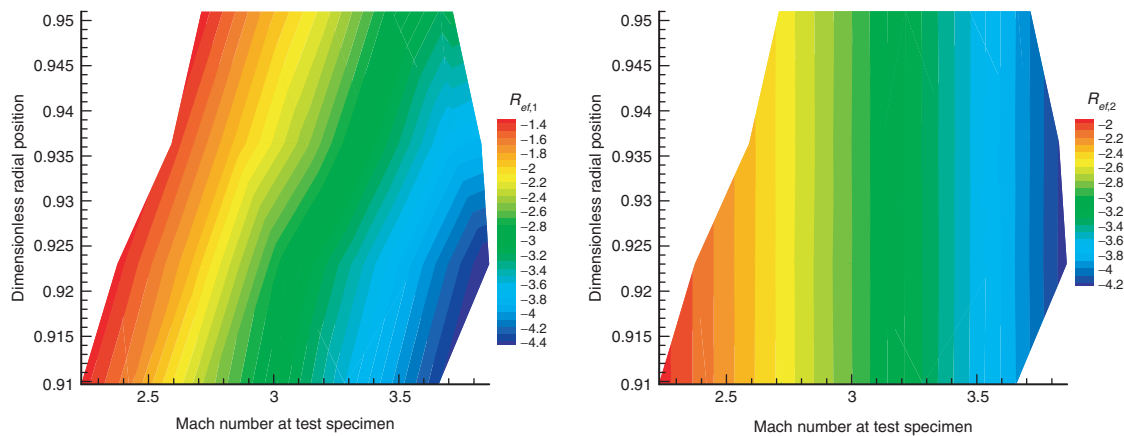


Figure 9. Contour plot of radial entropy factor as function of radial position and test specimen plane Mach numbers with slowdown.

The inlet temperature before the shock is assumed to be uniform. CFD study had already revealed that the angular velocity of rotation, Ω_r at any radius r vary as follows.

$$\Omega_r = \Omega_{ref} \times \left(\frac{r}{r_{max}} \right)^\delta \quad (12)$$

Ω_{ref} is the angular velocity in the test specimen plane nearest to the wall. It represents the slowed down angular velocity due to the presence of a test specimen (a stationary body) in the rotational flow field. Using the measured temperatures at inner and outer positions of body, it is possible to estimate the slowdown in the test specimen plane. When a gas at temperature T_i (position of “i” is shown in Fig. 2b) stagnates, its temperature rises. This stagnation temperature T_{oi} can be calculated using following equation:

$$\frac{T_{oi}}{T_i} = 1 + \frac{\gamma - 1}{2} M_i^2, i = 1, 3. \quad (13)$$

If T_1 and T_3 are the free stream temperatures corresponding to the inner and outer radius of the test specimen. T_{o1} and T_{o3} will be their corresponding stagnation temperatures at Mach numbers M_1 and M_3 . From the first assumption $T_1 = T_3$, Eqn. 13 can be written as

$$T_{o3} \left[1 + \frac{\gamma - 1}{2} M_1^2 \right] = T_{o1} \left[1 + \frac{\gamma - 1}{2} M_3^2 \right]. \quad (14)$$

$$M_i = \frac{\left[r_i \Omega_{ref} \times \left(\frac{r_i}{r_{max}} \right)^\delta \right]}{\sqrt{\gamma RT_i}}, \quad i = 1, 3. \quad (15)$$

This can be solved as:

$$\Omega_{ref} = \left[\frac{(T_{o3} - T_{o1}) 2\gamma RT}{(\gamma - 1) \left(T_{o1} r_3^2 \left(\frac{r_3}{r_{max}} \right)^{2\delta} - T_{o3} r_1^2 \left(\frac{r_1}{r_{max}} \right)^{2\delta} \right)} \right]^{1/2}. \quad (16)$$

The slowdown ($\Delta\Omega$) occurring at a position (radius r) in the cylinder can be written as follows.

$$\Delta\Omega = \Omega_{SB} - \Omega_{ref} \times \left(\frac{r}{r_{max}} \right)^\delta \quad (17)$$

The stagnation pressure of the body placed at radius r facing flow approaching with slow down Mach number M_r has been used to calculate the static pressure before the shock.

$$\frac{P_{stag}}{P_r} = \left(\frac{\gamma + 1}{2} M_r^2 \right)^{\frac{\gamma}{\gamma-1}} \left(\frac{\gamma + 1}{2\gamma M_r^2 - (\gamma - 1)} \right)^{\frac{1}{\gamma-1}} \tag{18}$$

It may be noted that M_1, M_3 given by Eqn. 14 and M_r used in Eqn. 18 refer to the slowdown Mach number at their respective positions.

Equations (9) and (11) are solved iteratively to determine δ parameter by minimization error. δ was obtained as,

$$\delta = \frac{M_{wall}}{2} \tag{19}$$

where M_{wall} is the Mach number of the cylinder wall at room temperature. This model was able to predict for all cases tested. The validity of this correlation is within the range of experimental data. The dimensionless radial position should be within 0.91 to 0.951, while wall Mach numbers should be within 4.9 to 6.6 for the correlation to be valid. Fig. 8 shows the radial entropy factor as function of test specimen plane Mach numbers with and without slowdown. The entropy generation rate changes appreciably with Mach number without slowdown, which is not expected. Whereas, $R_{ef,1}$ and $R_{ef,2}$ is plotted against the slowdown Mach number obtained from the above model shows all the data can be approximated to a straight line. The decrease of $R_{ef,1}$ and $R_{ef,2}$ with Mach number supports our claim that the physics of the problem at hand has been modeled with sufficient accuracy. Fig. 9 shows the contour plot of radial entropy factor as function of radial position and test specimen plane Mach numbers with slowdown. Figure 10 shows the test specimen tip position as a function of stagnation pressure test specimen plane Mach numbers without and with slowdown model. Fig. 11a,c,e and g show the various parameters of test specimen with slowdown model compared with its counterparts without slowdown model as shown in Fig. 11b,d,f and h.

Fig. 12a and 13a show the plots of experimental values, while Fig. 12b and 13b shows the relative error in estimating the temperatures. It was observed that present simulation was able to predict the temperatures on the test specimen within $\pm 2\%$.

Apart from the slowdown the upstream temperature and upstream pressure before the test specimen can also be predicted. Figure 14a and 14b show the predictions for mean temperature and pressure at upstream condition for various experiments studied.

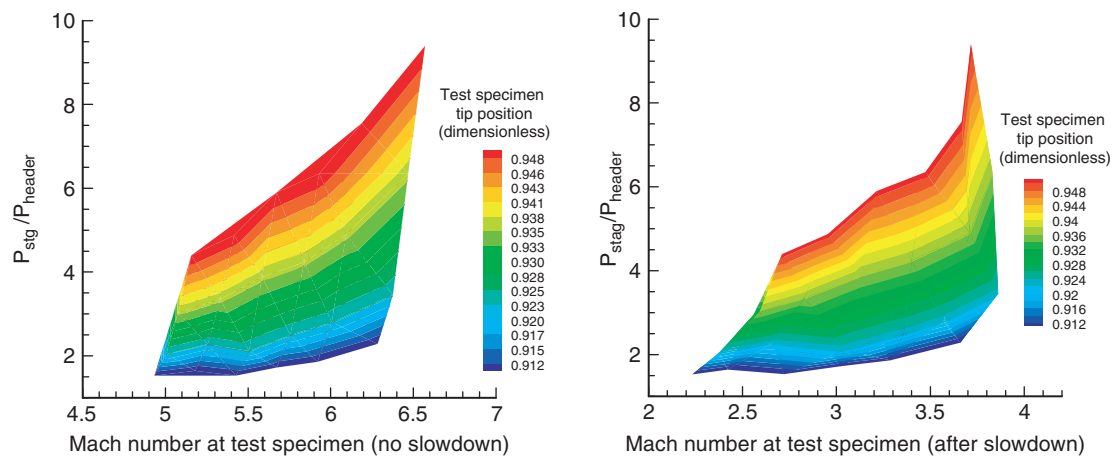


Figure 10. Test specimen tip position as a function of stagnation pressure test specimen plane Mach numbers without and with slowdown model.

Parametric Study of Stationary Body Facing its Own Wake in a High Speed Compressible Rotating Flow

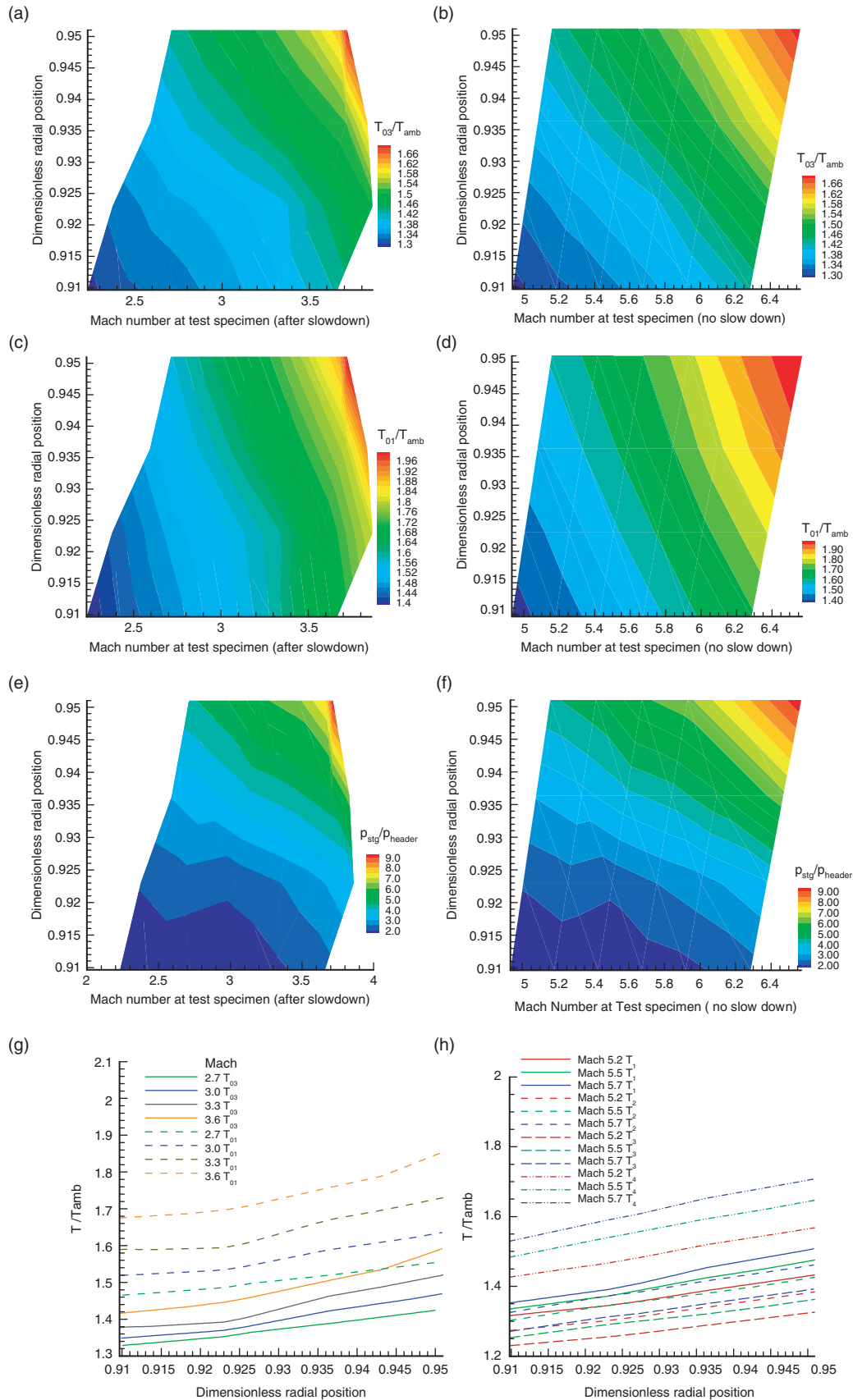


Figure 11. a, b, c, d, e, f, g and h shows various parameters of test specimen with slowdown model.

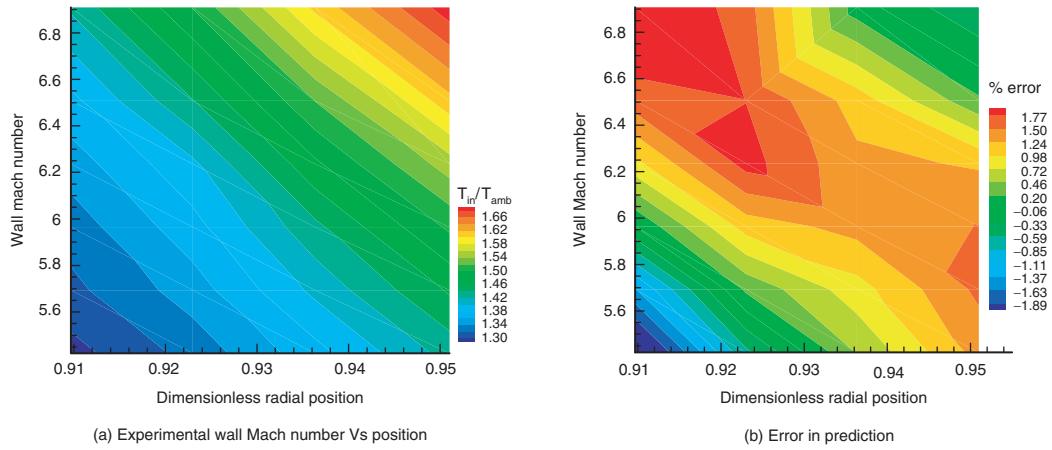


Figure 12. Experimental observations and error in prediction of Pitot inner tip temperature.

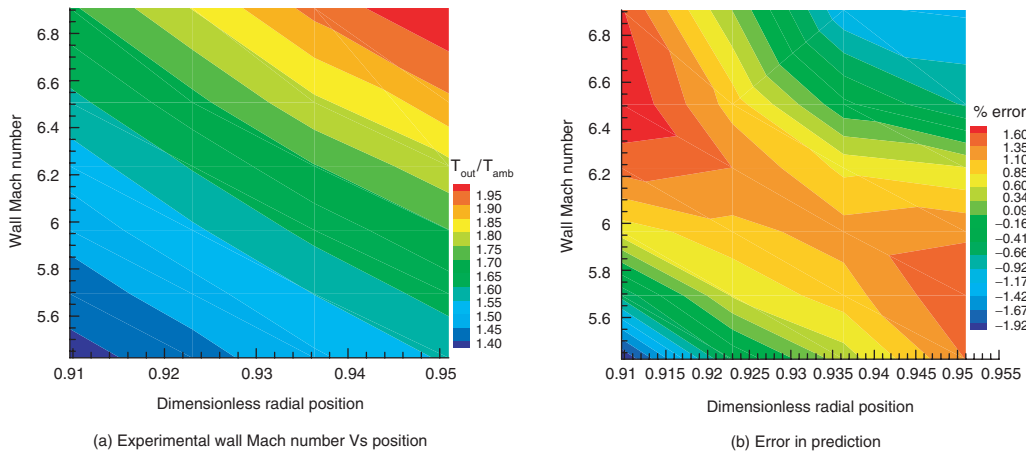


Figure 13. Experimental observations and error in prediction of Pitot outer tip temperature.

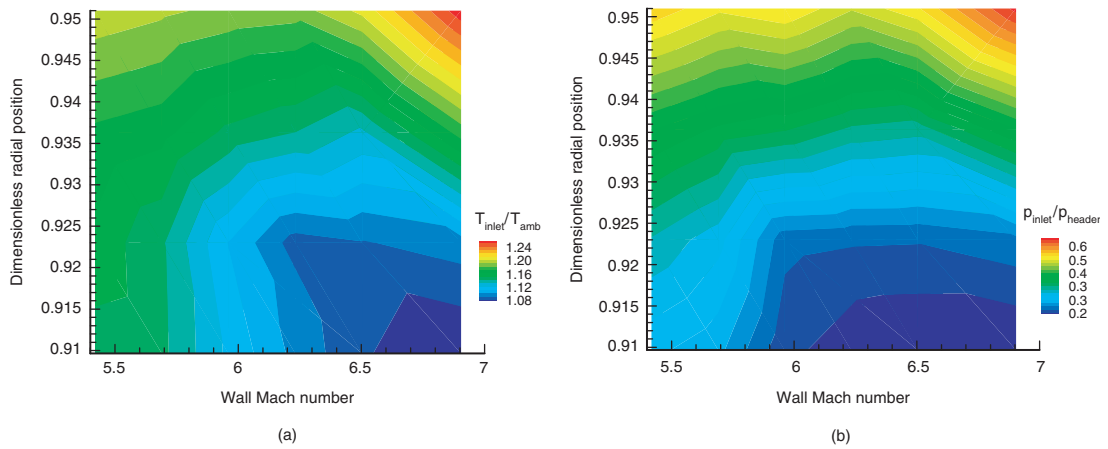


Figure 14. Predicted mean upstream temperature and pressures in the plane of test specimen.

5. CONCLUSIONS

The high speed rotating flow is characterized by exponential rise in density with respect to radius and the fact that the body faces its own wake makes the prediction of stagnation pressure and temperature quite complicated. CFD studies also revealed that the body wake causes slowdown of the flow. The experimental studies were conducted to carry out stagnation temperature and pressure measurements. Based on theoretical studies entropy term called radial entropy factor was developed to account for the entropy rise due to shock in a rotating flow environment. Radial entropy factor when plotted against the slowdown Mach number from the above model shows all the data following a unique curve. The uniqueness further supports our claim that the physics of the problem at hand has been modeled with sufficient accuracy. Based on CFD results and experimental study a mathematical model was also developed which was able to predict the slowdown, and the upstream properties of the high speed flow before the test specimen. The model also predicted the test specimen inner and outer wall temperatures within $\pm 2\%$ accuracy. Future scope shall include a more detailed study with different shapes with different material of construction of stationary body.

ACKNOWLEDGEMENT

Author is thankful for the encouragement and invaluable guidance provided by Prof. S. Banerjee. Author also acknowledges support provided by Mr. A.K. Kalburgi, Mr A.K. Mahendra, Mr M. Chatterjee, Mr G.N. Sashi Kumar and Mr Vinay Kumar during the course of this study.

REFERENCES

- [1] Bark, F. and Bark, T., On vertical boundary layers in a rapidly rotating gas. *Journal of Fluid Mechanics*, 1976, 78, 815–825.
- [2] Brouwers, J., On compressible flow in a rotating cylinder, *Journal of Engineering Mathematics*, 1978, 12, 265–285.
- [3] Rusanov, V.V., “A blunt body in a supersonic stream.” *Annual Review of Fluid Mechanics*, Vol. 8: 377–404, January 1976 DOI: 10.1146/annurev.fl.08.010176.002113.
- [4] Nilifard, R., Ahmadikia, H., “Supersonic Flow over a Blunt Body using the Direct Simulation Monte Carlo Method and Navier-Stokes Equations”, *Adv. Theor. Appl. Mech.*, Vol. 3, 2010, no. 2, 75–87.
- [5] Aoki, E., “Numerical Computations of shock wave behavior around a scoop by the MacCormack-TVD scheme”, In *Proc. Workshop on Separation phenomena in Liquids and Gases*, Charlottesville (Ed. H.G. Wood), 1992.
- [6] Aoki, E., and Suzuki, M., “Numerical studies on gas flow around scoop of a gas centrifuge” In *Proc. Sixth workshop on Gases in Strong Rotation*, Tokyo (Ed. Y. Takashima), 1985.
- [7] Matsuda, T., and Tamura, N., “Numerical Simulation of flow past scoops in a gas centrifuge”, In *Proc. Workshop on Separation phenomena in Liquids and Gases*, Darmstadt. (Ed. K.G. Roesner), 1987.
- [8] Matsuda, T., Tamura, N., and Sawada, K., “Three-dimensional numerical simulation of flows past scoops in a gas centrifuge”, *J. Fluid Mechanics*, 201, 1989.
- [9] Roberts, W.W., “Three dimensional stratified gas flows past impact probes and scoops: N-body, Monte Carlo calculations”, In *Proc. Sixth workshop on Gases in Strong Rotation*, Tokyo (Ed. Y. Takashima), 1985.
- [10] Mahendra, A. K., Gouthaman, G., and Singh, R. K., 2011, “Viscous Compressible Slip Flows. Part 2: Meshless Solver for Rotating Slip Flows,” *International Journal of Emerging Multidisciplinary Fluid Sciences*, 3, pp. 49–83.
- [11] Mandal, J. C., and Deshpande, S. M., 1994, “Kinetic flux vector splitting for Euler equations,” *Computers & Fluids*, 23(2), pp. 447–478.
- [12] Deshpande, S.M., “A second order accurate kinetic theory based method for inviscid compressible flow”, *NASA TP-2613*, 1986.
- [13] Vinay Kumar, Mahendra, A.K., Praveen, C., Gouthaman, G., “Rotating gas flow past stationary cylinder”, 14th Annual CFD Symposium, August 10–11, 2012, Bangalore, India.
- [14] Balachandran, P., “Fundamentals of Compressible Fluid Dynamics”, Phi Learning Pvt. Ltd, 1st Edition, ISBN: 8120328574, 2009.